Tracking 3-D Body Motion for Docking and Robot Control

M. Donath, B. Sorensen, G.B. Yang, and R. Starr
University of Minnesota
Minneapolis, MN 55455

1. ABSTRACT

A considerable number of activities require closed loop control of all six degrees of freedom of body motion. Accuracy and bandwidth are key issues in applications ranging from mirror positioning to robot control, from vehicular docking to autonomous construction and maintenance systems. One limitation has been the absence of a robust sensor capable of such measurement in a real time environment.

An advanced method of tracking three-dimensional motion of bodies has been developed. This system has the potential to dynamically characterize machine and other structural motion, even in the presence of structural flexibility, thus facilitating closed loop structural motion control. The system's operation is based on the concept that the intersection of three planes defines a point. Three rotating planes of laser light, fixed and moving photovoltaic diode targets, and a pipe-lined architecture of analog and digital electronics are used to locate multiple targets whose number is only limited by available computer memory. Data collection rates are a function of the laser scan rotation speed and are currently selectable up to 480 hz. The tested performance on a preliminary prototype designed for 0.1 in accuracy (for tracking human motion) at a 480 hz data rate includes a worst case resolution of 0.8 mm (0.03 inches), a repeatability of +0.635 mm (+0.025 inches), and an absolute accuracy of +2.0 mm (+0.08 inches) within an eight cubic meter volume with all results applicable at the 95% level of confidence along each coordinate region.

The full six degrees of freedom of a body can be computed by attaching three or more target detectors to the body of interest. Structural motions can be tracked by attaching targets to the specific points of interest. The accuracy in reducing XYZ target position data to body angular orientation for this first prototype ranges from +0.5 to +1.0 degrees. Moving targets can be tracked at speeds exceeding 1 m/s with signal integrity tested but not limited to 25 Hz motions.

2. INTRODUCTION

Sensors that track body motion are critical to the implementation of closed loop position control systems in addition to facilitating the analysis of system dynamics. Many potential applications exist, from the analysis of human motion to the control of robot motion. Positioning accuracy and fast response of robot end-effector motion are important for many applications. While industrial robots have acceptable repeatability, their absolute positioning accuracy is relatively poor. This is for the most part due to their control architecture which involves closed loop position control at the joint level rather than at the end-effector level. There has been a need to accurately track the full 6 degrees of freedom of end-effector motion in order to facilitate what is known as end-point control (9). To enhance robot performance, a number of instrumentation systems have been developed for measuring 3D body motion in particular for the study of human movement. These include systems based on photogrammetry, electrogoniometry, sonic triangulation, accelerometry, and electro-optical phenomena. During the last decade, particular attention has been focused on electro-optical techniques. Within this group are several systems currently used in human motion laboratories: VICOM, SELSPLOT, CODA-3, and the United Technologies systems. Each system quotes comparable performance characteristics sufficient for the purpose of collecting human motion data, but each has inherent limitations in the maximum number of targets, in data processing time, in accuracy, or in bandwidth, which thus limit their utility to other applications. Other systems (2,7) have been developed for performance measurement of robot function but these are typically not compatible with closed loop control oriented sensing. Those that are (3) have other constraints.

The system described here, the Minnesota Scanner (or MnScan), has been under development for several years in an attempt to provide a cost effective, high performance alternative. Our present prototype, which was developed for tracking human motion with a goal of achieving 0.1 inch accuracy per axis for all three dimensions, has undergone extensive testing and calibration. Figure 1 shows the physical layout of the laser scanning system in our Motion Analysis laboratory. This paper reports on our most recent results which demonstrate this system's potential for serving as a robot end point sensing system.
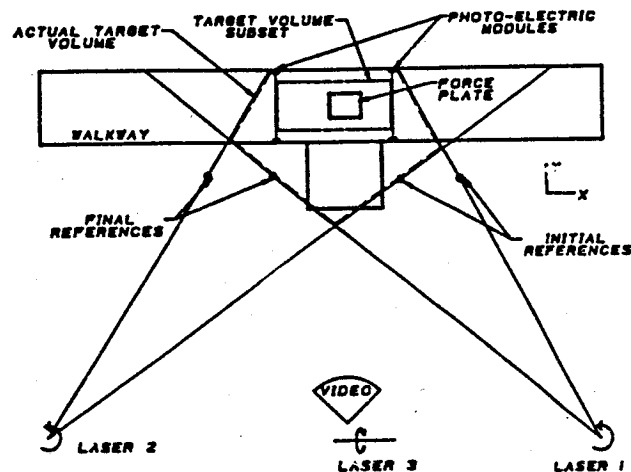
TOP VIEW
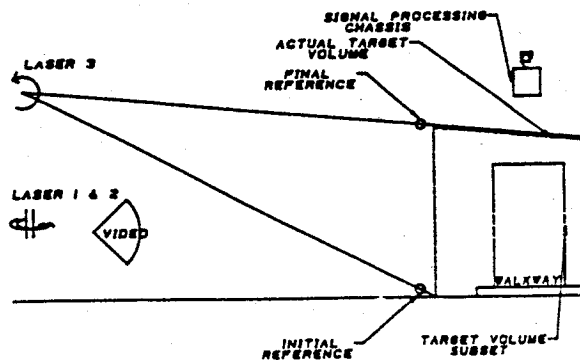
SIDE VIEW

Figure 1: Physical Layout of the Laboratory

3. SYSTEM CONFIGURATION

The system is based on the concept that three planes of light, with differing normal vectors, intersect at a point in three-dimensional space. The basic premise of the method is that three intersecting planes define a point provided that none of the directional cosines of the three planes are the same. Thus, if the equations of three planes are known, the intersection point's coordinates can be found.

The planes are generated by passing light from a low power laser through a cylindrical lens arrangement and are swept through the measurement field at a constant velocity by reflecting the plane off of a mirror rotating at a constant angular velocity. The mirror is an octagonal prism attached to a 60 Hz reluctance synchronous motor. This allows for a high data collection frequency, 480 Hz, and precludes the need for phased lock loops and connections between the motors. As the plane moves through the work cell, it passes over photodetectors sensitive to the laser's wavelength. The signal from each detector is filtered to remove background light, amplified, and then further conditioned to provide a TTL pulse each time a plane passes over it. In our present configuration only one laser is in the volume at any one time. This is done by phasing the three mirror scan motors appropriately. This phasing, its effects, and other design issues, are discussed in more detail in MacFarlane, 1983 (5) and MacFarlane and Donath, 1985 (6).

In order to tell the lasers apart, three fixed initial references are located at one corner (lower right front) of the field so that each of these detectors views only one laser. The pulses generated by these three detectors form the basis for the data collection scheme. Every time an initial reference signal changes to positive, a counter is reset. These signals provide the data board with the current laser status so data can be routed correctly. In addition to the initial references, there are also three fixed final references which define the opposite end of the target volume and a number of target detectors, which are free to move within the

target volume. The final reference detectors are not necessary but provide a means for compensating for any small deviations in the angular velocity of the mirrors, if necessary. Although closed loop speed control of the motors is possible, it was deemed unnecessary, given the present configuration and the desired specifications.

To locate a point in three dimensions, the following pieces of data are required; the equation of the plane when it passes the initial reference, which is assumed to be known, and the angle of rotation from the initial reference to the target for each of the three planes. The angle information is generated by sending the TTL conditioned signal from each detector to a data collection board. This board contains four major sections:

1. A 16 bit counter driven by an eight MHz quartz crystal.
2. A signal decoding section.
3. A bank of registers: 3-16 bit registers for each target detector and final reference detector.
4. A section to decode the register address for output.

and four register buses;

1. Memory input.
2. Enable to read.
3. Enable to write.
4. Memory output to parallel port.

Each time a detector "sees" a plane, the current counter value is placed in the appropriate register as determined by the signal decoding section. This is done continuously, transparent to the host processor every time a plane passes through the target volume. The value in the register represents the data board time for the plane to rotate from reference to target, and can be converted to an angle since the angular velocity is constant.

4. TARGET CONFIGURATION

Target photodetectors were selected to have high sensitivity in order to minimize needed laser power, and had a 120 degree wide angle field in order to be visible to all lasers as they moved in the field. The active area of the sensor was 20 mm^2.

As stated, each target detector defines a point in space. To define the orientation of a body, three points are required. A fourth point provides redundancy in the event that one detector is momentarily blocked from the view of the light planes, and also allows a least squares estimate to be fitted based on 4 sets of three points. The greater the separation distance between targets, the greater the accuracy in determining the body orientation. However, in order for the target mounts not to get unwieldy, the separation distance was constrained.

5. SYSTEM CONFIGURATION EFFECTS ON COMPUTATION

After the timing data has been obtained it must be converted to three-dimensional position information (points) in order to be useful. To locate each point the information required is the location of the axis of rotation of the plane, the location of the initial reference, and the angle of rotation from the initial reference to the target for each plane. With this information, each plane can be represented at the target, and the intersection of these planes define the target's (x,y,z) location. The exact equations can be found in Sorensen, 1986 (12).

In order to compute a target's location, the locations of the reference targets and the optical axes of rotation must be known. The axes of rotation are positioned so that they are parallel or orthogonal to each other and to the global coordinate system (GCS), with two axes being vertical and the third, horizontal in orientation. This is done to simplify the position calculations. The simplification is necessary in order to decrease the computational time required of data reduction. Bechtold (1) showed that if the axes of rotation were arbitrarily located, the solution process would be an open form iteration. To obtain a solution, all three angles are entered into the solution matrix along with an initial approximation for the solution. A Newton iteration method is then used to converge to the final solution. However, by orienting two of the light planes along a vertical orientation, their intersection yields a vertical line. This line defines the coordinates of the point in the horizontal plane. To define the third coordinate, the third plane is used to intersect the vertical line. The solution process in this case is closed form in nature and very short; only two equations. The derived solution in this case is thus reduced to two two-dimensional calculations per three-dimensional point. The time saved is immense and makes the process feasible for real-time situations.

6. DETERMINATION OF SYSTEM PARAMETERS

As indicated earlier, the location of each axis of rotation must be determined in order to effectively use the system. Other parameters that must be identified are the location of the initial and final reference photodetectors for each laser. To locate the positions of the six fixed reference diode targets and a local coordinate frame for each moving axis of rotation, a ZEISS precision measurement system was used. This measurement device consists of two theodolites interfaced to a computer. Once the theodolites are calibrated to provide their locations with respect to a global coordinate frame in the room, points can be located with respect to the defined frame with accuracy and repeatability better than 0.003 inches.

To do the system calibration, four or more points of known location are needed to calibrate the theodolites. These points were located on an optical bench (2m x 2m) which straddled the target volume during the calibration process (see Figure 2). This removable test bench was used to define the global coordinate system and to set up the ZEISS calibration points which were located with a six-foot vernier caliper. After the reference detectors
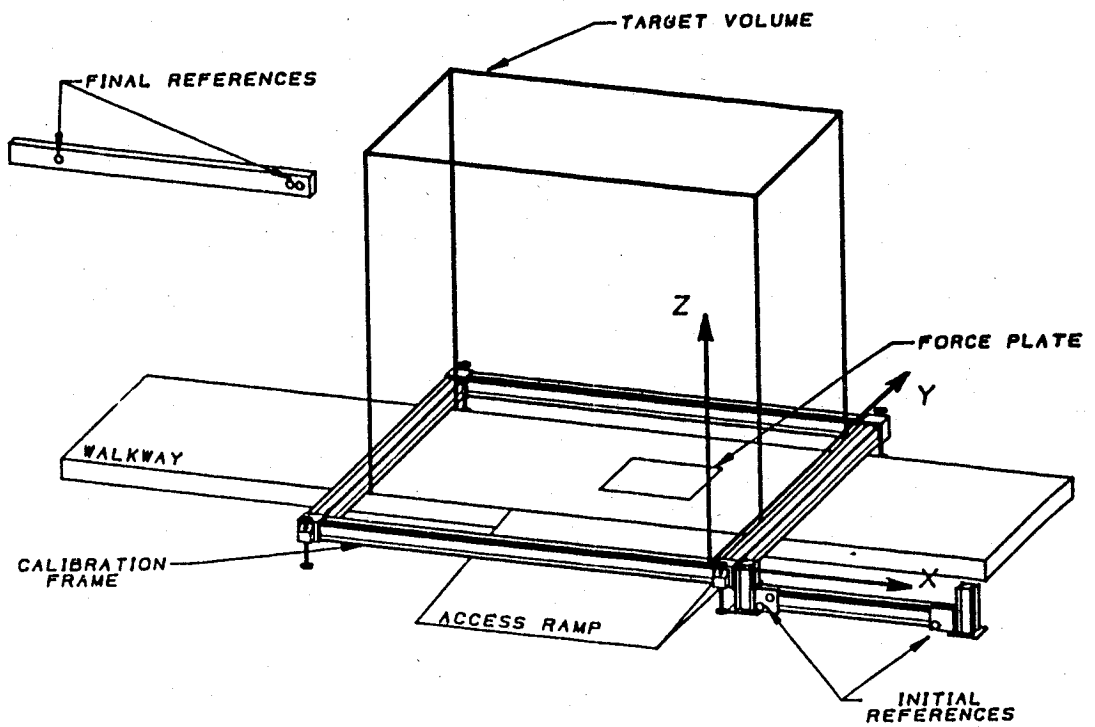
33

Figure 2: Target Volume as Defined by the Inertial References and the Global Coordinate System
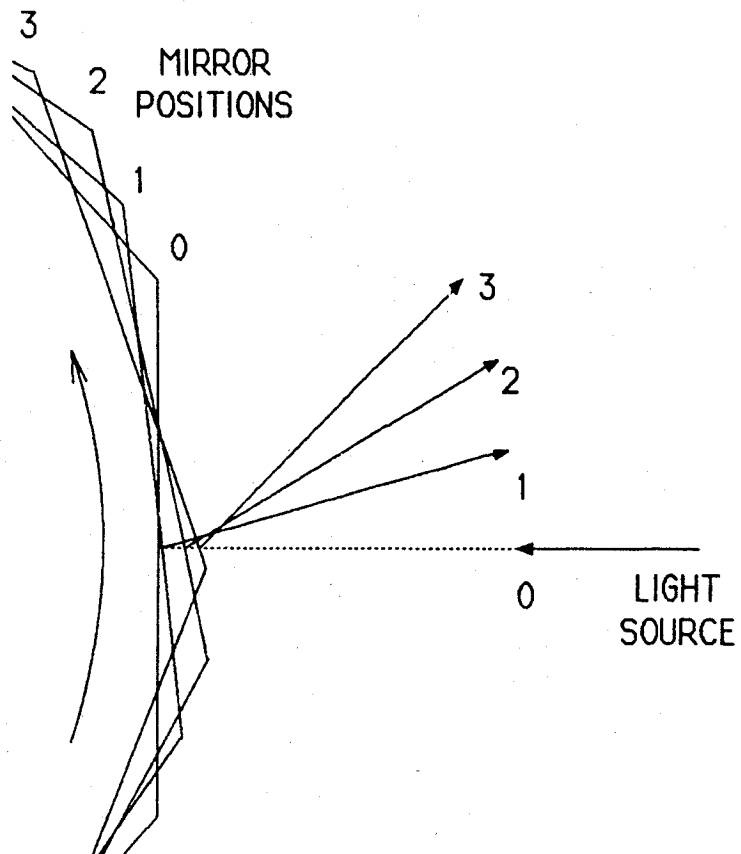

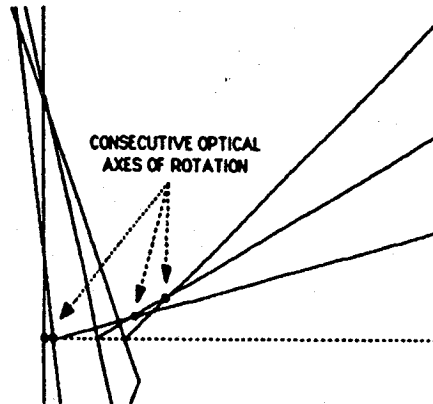Figure 3a: Magnified View of Three Reflected Light Planes

Figure 3b: Blowup of Region Adjacent to Moving Mirror

are affixed to the measurement field boundaries and the axes of rotation oriented, the three mechanical axes of rotation and the six reference detector locations may be measured. With all system parameters defined, the data generated by the system can be reduced to three-dimensional points.

7. MOVING AXIS OF ROTATION

Although the use of the octagonal mirror gives the system a high bandwidth, it introduces a complication. Since the reflective surface is a finite distance from the mechanical axis of rotation, the optical and mechanical axes are not coaligned, and as a result, the optical axis is not fixed in space, but moves as the mirror rotates (see Figure 3). This motion is not negligible and cannot be ignored since the axis can move as much as 0.25 inches in each direction perpendicular to the axis of rotation. Fortunately, this motion is a function of realizable parameters and can be fitted to an equation. The determining factors are the geometry of the mirror and the line defined by the incident laser beam. A detailed model was derived from differential geometry and implemented in software (12).

8. STATIC PERFORMANCE TESTING

To determine if the data generated by the system is accurate, a detailed calibration was performed. The process involved moving a vertically-oriented, linear array of eight targets through the target volume.

The optical bench was used as a means for mounting and providing regular movement of the target configuration. A movable horizontal rail was placed parallel to the x axis to yield changes in y. Displacement of a vertical rail with the attached target configuration yielded changes in x. With the eight targets at varying heights, it was not necessary to change the z component. The targets were moved along six inch intervals in the x and y directions by the appropriate adjustment of the horizontal and vertical rails. This protocol yielded data on 616 discrete points within the target volume; eleven locations in the x direction, seven in the y, and eight in the z.   At each location, data was recorded using both systems; the theodolite based method and the Laser Scanning approach. Each target was sampled (measured) 200 times by the Laser Scanning system to provide data for statistical analysis.

9. RESULTS

Accuracy: In testing the system a phase lag error was discovered. By modeling the error, based on a smaller subset (200 out of 616) of the total measurement, the phase lag was eliminated. The spatial locations of the detectors for the ZEISS and the MnScan system are shown in Figure 4 for 3 slices through the field. It can be seen that on the scale of these plots, the data from the two systems effectively superimpose. However, further analysis shows that there was a root mean squared error of 0.04 inches that remained and that a 95 percent confidence interval includes an error of ±0.08 inches along each axis. These results were obtained at 480 Hz data acquisition rates. (Two data points are missing from Figure 4 because their associated data file was irretrievably lost by an inadvertent deletion. These were thus not included in any error or calibration analyses.)

10. RESOLUTION

The spatial resolution is dependent on the position within the target volume. The input parameters to the solution matrix, the three rotation angles, have an angular resolution; thus, the distance from the target to each laser affects the tangential resolution of each laser.

Each angle has a resolution determined by the angular velocity of the mirror and the clock speed on the data collection board. The angular resolution is the amount of rotation per clock count. For the present configuration, with an eight faceted mirror rotating at 60 Hz and an eight MHz clock, the resolution is:
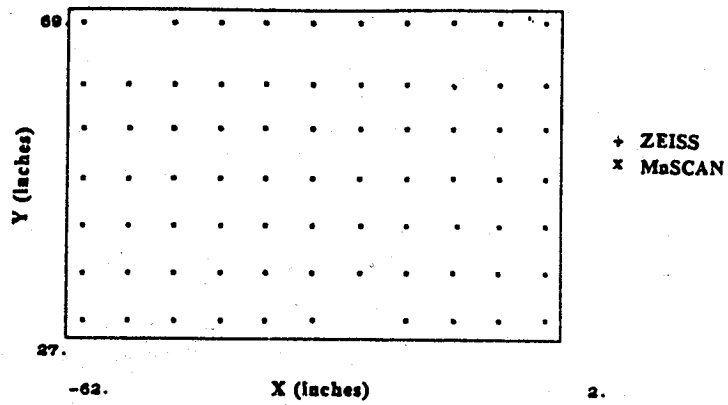
Figure 4a: Plot of Actual and Measured Points in the XY Plane After the Angular Correction
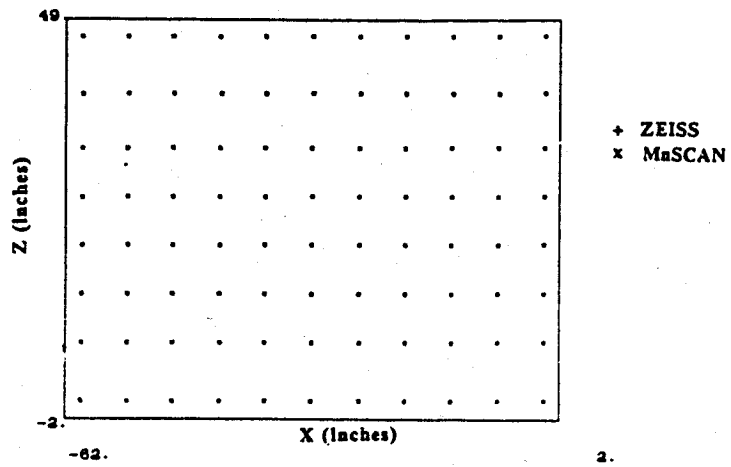

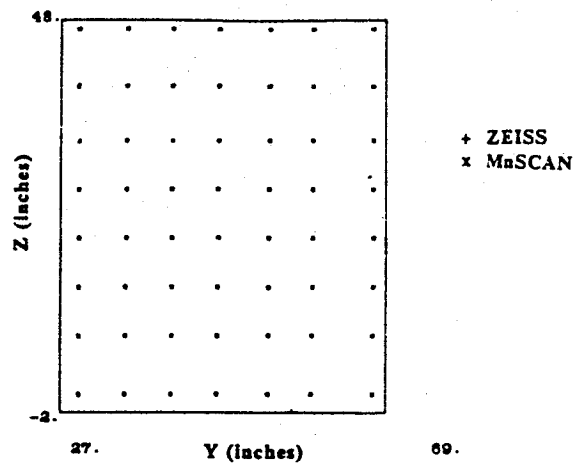Figure 4b: Plot of Actual and Measured Points in the XZ Plane After the Angular Correction

Figure 4c: Plot of the Actual and Measured Points in the YZ Plane After the Angular Correction

36

$$\frac{\left(90 \dfrac{\text{degrees}}{\text{facet}}\right) \times \left(8 \dfrac{\text{facets}}{\text{revolution}}\right) \times \left(60 \dfrac{\text{revolutions}}{\text{second}}\right)}{8\,\text{E6} \dfrac{\text{counts}}{\text{second}}} = 0.0054 \frac{\text{degrees}}{\text{count}}$$

At a distance of 30 feet (the maximum target distance for any laser) the angular resolution corresponds to a tangential resolution of 0.034 inches. This result is misleading because it is not the spatial resolution. By using the tangential resolution and the system's geometry, the actual spatial resolution at a point can be determined. This resolution has components along each of the three different axes which varies from half to two-thirds of the tangential resolution of 0.034 inches across the measurement field.

11. SIGNAL TO NOISE RATIO: POWER SPECTRAL DENSITY

Noise in the signal comes from a variety of sources including electronic, optical and environmental effects. If one were to examine the timing data from a stationary detector for one laser, the expected result, assuming no noise, would be a constant number. The actual result varies from five to ten counts depending on the angular location within the field; the closer to the initial reference the smaller the variation. To determine the impact of this noise, data was collected at 480 Hz to allow processing by a 10-bit FFT (Fast Fourier Transform) for signal decomposition. The resulting frequency magnitudes displayed a single spike at zero hertz and no signal elsewhere. To observe the low level noise the zero hertz value was reset to zero and the magnitudes were replotted (see Figure 5). Now, peaks appear at 60 and 120 Hz with the 120 Hz peak having a magnitude 0.03 percent of the zero hertz magnitude. This result is the same throughout the field for each plane of light, independent of detector and signal processing channel. We have identified the source of the 60 Hz noise and are working towards eliminating it.
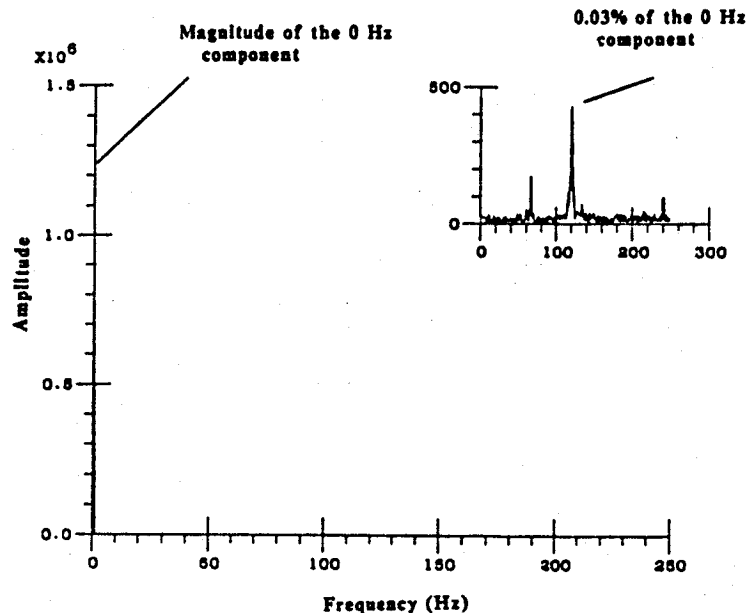

Figure 5: PSD of a Timing Signal

12. SCATTER PLOTS AND NOISE FILTERING

To examine the noise effects on accuracy and resolution, a set of data (300 samples at 480 Hz) for a stationary target was collected and reduced to (x,y,z) coordinates. This data is represented in two planar projections, an (xy) plane view and a (yz) plane view. The (xz) plane is not used because x and z are independent and the plot of this plane would just show up as a cloud of points. An important fact to remember is that the active area of the detector is 20 mm^2, or 0.176 inches in the x and z directions. The results indicate that all calculated points fall within the active area.

The planar projections (Figure 6) show the effect of the 5 to 10 counts of noise at a particular spatial location within our field. In both projections patterns are visible. For the (xy) plane, clusters located at the intersections of a diamond shaped grid are evident. This happens because the rotating light planes from lasers one and two pass the detector at discrete values associated with the clock resolution. The diagonal lines of the grid represent the orientation of the light plane at each discrete value. The small clusters in the (XY) scatter plot are due to a variety of effects that are beyond the scope of this paper. Suffice it to say that they are not a function of motor speed or motor phasing and are thus not easy to remove at their source. Nevertheless, despite this noise, the resulting error over the test region falls within + 0.08 inches at the 95% level of confidence, well within the design specs for this prototype.
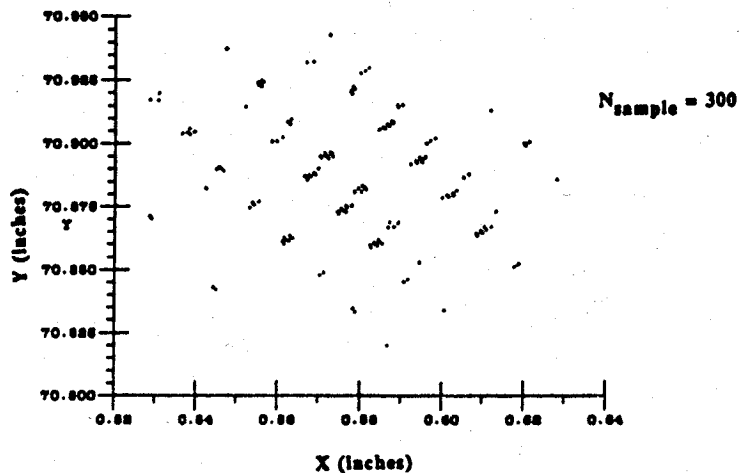
37

$N_{sample} = 300$

Y (inches)

X (inches)

Figure 6a: Scatter Plots of the Signal Noise Effects in the (XY) Plane

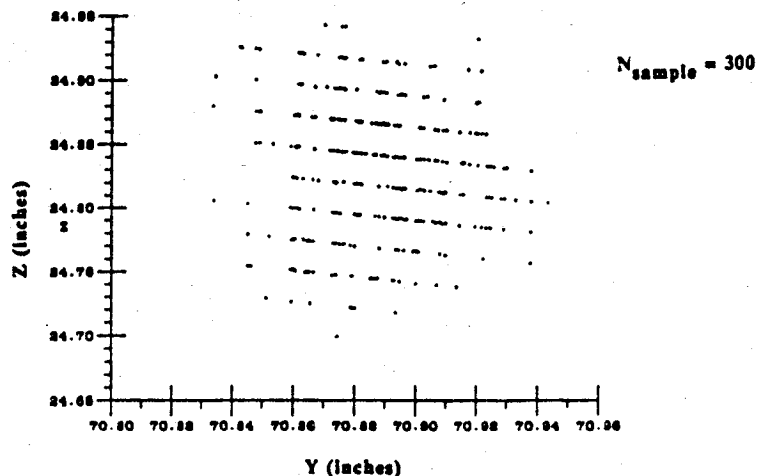$N_{sample} = 300$

Z (inches)

Y (inches)

Figure 6b: Scatter Plots of the Signal Noise Effects in the (YZ) Plane

Although these projections show the locations of each digitized point, no information on relative density is obvious because multiple points are superimposed. This is important because in the (xy) projection of Figure 6 only 20 percent of the data points are visible. To determine the distribution of the computed position, a two dimensional histogram of the (xy) scatter plot was made. The area was divided into equal regions such that groupings were preserved, and the number of points in each cell was totaled. This data was then plotted in order to produce the histogram in Figure 7. This graph shows that the points indeed distribute themselves along quantized laser planes.

To examine low pass effects on the accuracy and repeatability, the timing data can be passed through a digital filter. The filter used was a tenth order Butterworth lowpass with time reversal to preserve phase. To prevent start up oscillations, the first half of the signal is folded and inverted about the beginning of the signal and likewise for the second half of the signal. This allows smooth transition signals and any start up disturbances should die out in the artificial portion of the signal. To provide design variability, the -3db cut-off level can be specified to achieve the desired performance. To eliminate the 120 Hz peak, a 100 Hz -3db cut-off filter can be used. Each of 27 sets of modified timing data was passed through a filter and then rounded off to preserve the discrete nature of the data for this example. At this point the filtered timing data can be reduced to coordinates and plotted. These results (Figure 8) have the same patterns as before but now the noise has been attenuated, as expected. Although the noise has diminished, the signal to noise ratio can be improved even further if desired. The result of using a filter with a -3db cut-off level of 40 Hz is shown in Figure 9. The histogram indicates that the filter reduces the group of points to within a range of 0.04 inches in the x and y directions or an error of ±0.02. The same process yields a range of 0.06 inches in the z direction (error of ±0.03).
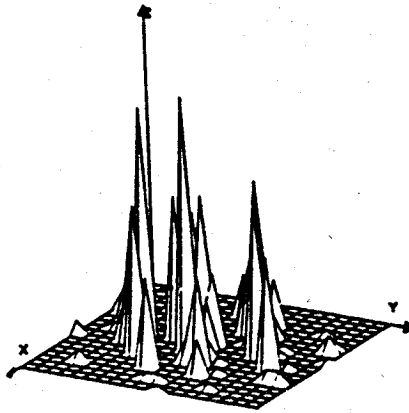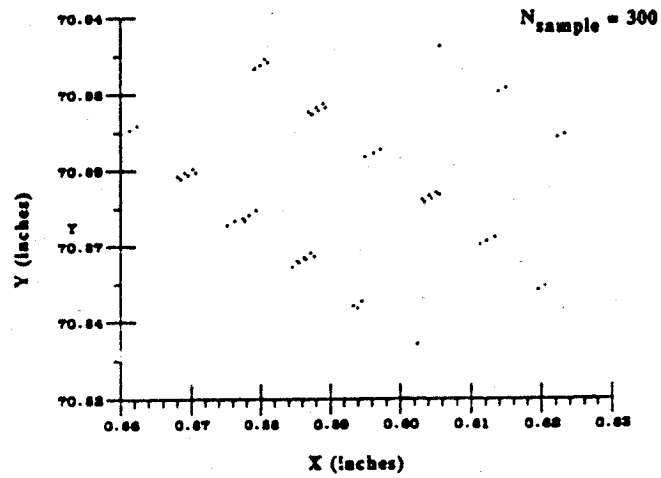
38

Figure 7: Histogram of (XY) Plane Scatter Plot

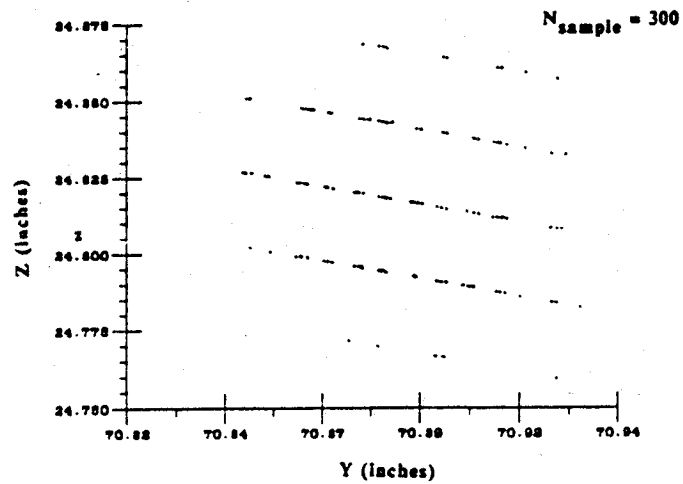Figure 8a: Scatter Plots of the Signal Noise Effects in the XY Plane with a 100 Hz Low-Pass Filter

Figure 8b: Scatter Plots of the Signal Noise Effects in the YZ Plane with a 100 Hz Low-Pass Filter
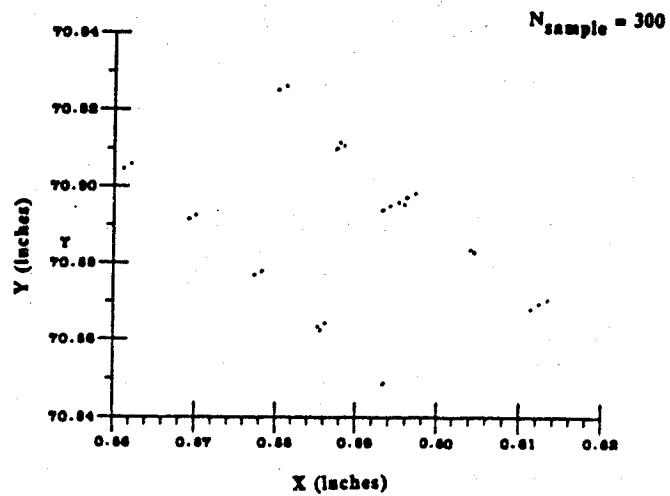
39

$N_{sample} = 300$

Figure 9a: Scatter Plots of the Signal Noise Effects in the XY Plane with a 40 Hz Low-Pass Filter
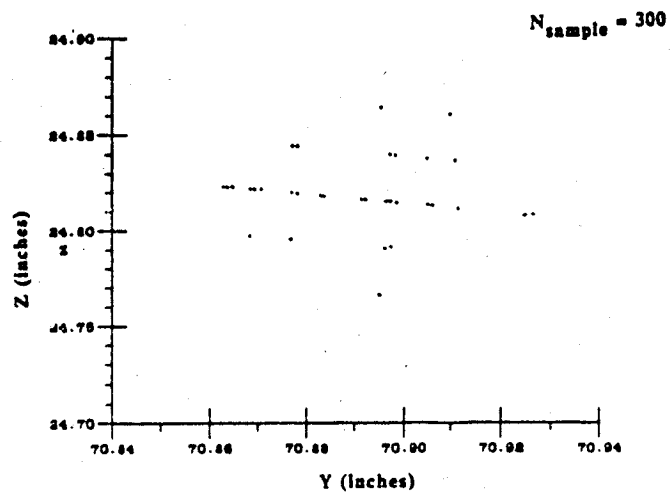
$N_{sample} = 300$

Figure 9b: Scatter Plots of the Signal Noise Effects in the YZ Plane with a 40 Hz Low-Pass Filter
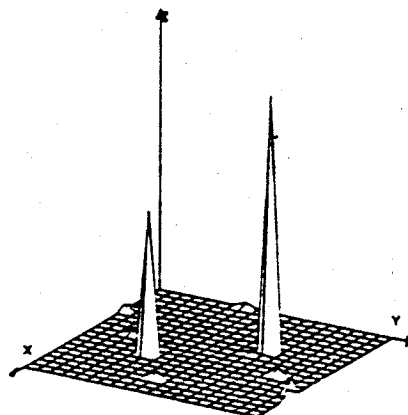

Figure 9c: Histogram of (XY) Plane with a 40 Hz Low-Pass Filter

40

13. DYNAMIC TESTING

Two additional tests were implemented to test the system's performance. The first test considered a single pendulum supporting the eight targets on a 1.75 meter bar. The resulting low frequency motion covered an entire planar section of the target volume in an oscillatory pattern. Data was collected at frequencies from 60 to 480 Hz and showed, as expected, that there were no local discontinuities or global warping within the target volume.

The eight targets were placed at relatively regular intervals along the bar with the farthest being about 72 inches from the pivot point. The targets were in a linear configuration to achieve the effect of concentric circles. The advantage of this configuration is that the angular position, with respect to the center (or the axis) of rotation, is the same for each detector. This fact was used in two separate analyses of the pendulum data.

The first test was a simple plot of the points reduced from the timing data (no filtering). Since the motion was in the (xz) plane, only two axes were used for the plots. In the two cases displayed (Figure 10), the sampling frequencies were 120 and 480 Hz. Other sampling rates were observed but, since the results were similar, only these two are shown. On these displacement records, the concentric arcs are clearly evident. At this point, inspection of these graphs tends to support that there are no irregularities in the target volume. Furthermore, the arcs traced out in the 480 Hz case are sharply defined and very smooth, which indicates that the signal noise is indeed small in the global sense. In the 120 Hz case, the arcs are still very smooth, but not as sharply defined. This is partly due to the longer sampling period and, thus, multiple swings of the pendulum. The small effects of signal noise and the dynamics of the pendulum and its mount are more than enough to cause this blurring. The dark spots are the places where the pendulum changes direction; the deceleration and then acceleration puts the pendulum in one place for a longer time, thus causing the sampling density to be higher in these locations. Since there is friction in the pin joint, there will be damping of the motion; this is reflected by the decreasing amplitude of each swing.

A second method of analyzing the pendulum data was to plot the computed angular position of each detector with respect to time. This method produced excellent results and is described in Sorensen, 1986 (12).

The second test was to determine performance under small displacement and high frequency conditions. A single target was attached to the end of an aluminum rod, whose other end was mounted on the shaft of a closed loop position controlled DC servomotor. The proportional controller applied an oscillatory signal to the target tipped rod at specified frequencies. Incorporated in the feedback loop was a high resolution encoder, which provided an accurate angular displacement measurement independent of the MnScan generated data.

A more detailed description and analysis of this test in which the target was driven at frequencies from 0.5 to 25 hz, and both the target photodetector and the encoder were monitored, is also contained in Sorensen, (1986) (12).

Although further work is necessary, the implication thus far is that this system can record higher frequency dynamic deflections which can be used for the dynamic analysis of manipulators or ultimately for closed loop end-point control.

14. RELATIVE ORIENTATION BETWEEN ROBOT LINKS

One of the motivations in developing this system is to measure the 3-D rotational and translational displacements of one body with respect to another. This information is significant to a number of areas, e.g., tracking the 3-D motion of human joints. It also has been shown that dominant compliance in robots may come from the joints rather than from structural deflection in the links. Thus, the system was used to determine the 3-dimensional joint angles associated with relative motion of two bodies about a moving axis of rotation. These can be obtained based on the premise that three or more points define the position and orientation of a "rigid" robot link.

There are many ways of reducing sets of position data to orientation information, one of which is the SCHUT algorithm (4,10,11). This is a position averaging technique which provides the relative change in position between two bodies. The method used in our system is quite similar, but instead of using position averaging, it averages the orientation to reduce error and to determine changes in orientation. The results from the two methods agree within one degree in most of the cases tested.

To check the accuracy in determining these angles, a single degree-of-freedom jig was designed with each of the two links holding a cluster of four targets fixed with respect to each other. By displacing the jig throughout the measurement volume with the hinged joint angle fixed, the computed orientation angle based on the measured target locations can be compared to the actual angles. This was done for a range of angles for each of the three planes. The results of this test placed the error of the measurement at $\pm$ 0.5 to 1.0 degree at the 95% confidence level. The result represented the accuracy in predicting the relative orientation angle throughout the entire target volume for each of the three planes. Increasing the accuracy in the determination of the XYZ locations of targets, changing the relative locations of the targets in the cluster, and moving the target cluster further from the axis of rotation would improve this result significantly.

Calculation of the "instantaneous" axis of rotation of the joint in question is possible. This measurement can be performed on the system using the reduction algorithms (i.e., SCHUT), but is not entirely stable due to the nature of the computation. This is especially a problem with robot links oriented 180° relative to each other. A new and different method of calculating the orientation between two arms has been developed based on duality theorems and spatial kinematics (9). This method bypasses the instability conditions in other algorithms and thus provides a more accurate result for the rotation angles and the axis of rotation.
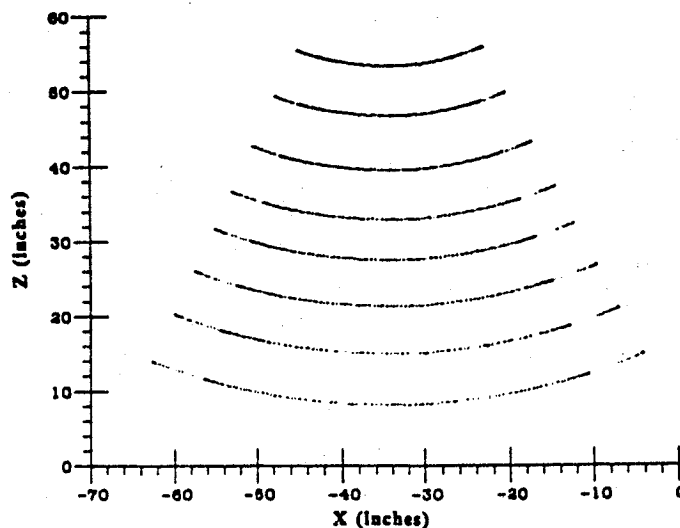
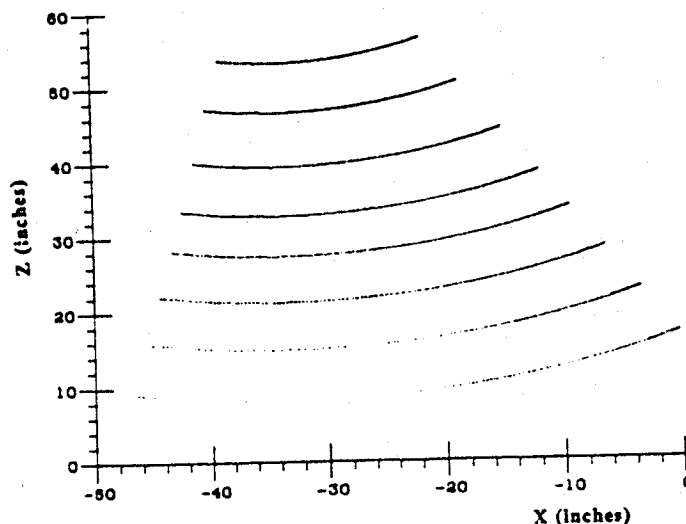Figure 10a: Cartesian Position Plot of the 120 Hz Case

Figure 10b: Cartesian Position Plot of the 480 Hz Case

15. CONCLUSION

The system described provides a fast and accurate method to record human locomotion and end-effector motion parameters. The tests reported here were conducted on the initial prototype pending the imminent completion of a newer system. The earlier prototype is only capable of tracking eight targets; thus data is available only for one joint. The system displays good dynamic bandwidth and acceptable performance. Data collected for 1.75 seconds at 240 Hz for 2 limb segments in a human motion study (4 target per limb) can be reduced to 3-D relative orientation or joint angles on our existing prototype in approximately 20 seconds on an Intel 8086 based system using code generated by a Fortran compiler (with no attempt at optimizing the code). This implies that a computation for a set of instantaneous orientation angles takes approximately 50 msec. A very preliminary test with an array processor has shown that this figure can be cut at least in half.

The accuracy of this system has surpassed the goal specification for human motion tracking for which it was originally designed; our goal had been to design a system with 0.1 inch accuracy. The system is not yet sufficiently accurate for use as an end-point sensor in the control of existing robot manipulators. We, however, do feel that the system can already be used for facilitating quite a number of experiments in this field.

42

Although the system requires line of sight for operation, the number of light sources and detector targets can be increased to ensure line of sight in most instances. Furthermore, when obstructions to the line of sight are unavoidable, full recovery is achieved as soon as the obstructions are removed.

The resolution of the MnScan system is only a function of the system clock and laser scan speed. The system accuracy at present reflects certain additional phenomena which are being isolated and investigated. Significantly better performance is planned for our next prototype.

16. ACKNOWLEDGEMENTS

17. REFERENCES

1. Bechtold, J. E., "Three-Dimensional Laser Scanning System with Application to Gait and Robotics," M.S. Thesis, University of Minnesota, August, 1983.
2. J. Chen and L. M. Chao, "Positioning Error Analysis for Robot Manipulators with All Rotary Joints," IEEE International Conference on Robotics and Automation, San Francisco, 1986.
3. A. Dainis and M. Juberts, "Accurate Remote Measurement of Robot Trajectory Motion," IEEE International Conference on Robotics and Automation, Saint Louis, 1985.
4. Lenox, J. B., and J. R. Cuzzi, "Accurately Characterizing a Measured Change in Configuration," ASME Paper No. 78-DET-50, 1978.
5. Macfarlane, J. F., "A System for Tracking Motion in Three-Dimensional Space," M.S. Thesis, University of Minnesota, June, 1983.
6. Macfarlane, J. and M. Donath, "Tracking Robot Motion in Three-Dimensional Space: A Laser Scanning Approach," Proceedings of the Nato Advanced Study Institute on Robotics and Artificial Intelligence, Italy, 1983; in M. Brady, L. A. Gerhardt, H. F. Davidson (ed.), Robotics and Artificial Intelligence, Springer Verlag, 1985.
7. Mooring, B. W. and T. J. Pack, "Determination and Specification of Robot Repeatability," IEEE International Conference on Robotics and Automation, San Francisco, 1986.
8. Peterson, S., "Kinematic Analysis of The Human Joint," Ph.D. Thesis, University of Minnesota, Fall, 1985.
9. Schmitz, E. and Cannon, R. H., "Further Experiments in the End-Point Control of a Flexible One Link Robot," to appear in ASME Journal of Dynamic Systems Measurement and Control.
10. Schut, G. H., "On Exact Linear Equations for the Computation of the Rotational Elements of Absolute Orientation," Photogrammetrias, Vol. 17(1):34-37, 1960-61.
11. Schut, G. H., "Formation of Strips for Independent Models," Photogrammetric Engineering, Vol. 34(7):690-695, July 1968.
12. Sorensen, B., "A Laser Scanning System for Tracking Three Dimensional Motion of Human Gait," M.S. Thesis, University of Minnesota, 1986.